Research Square

Preprints are preliminary reports that have not undergone peer review.
They should not be considered conclusive, used to inform clinical practice,
or referenced by the media as validated information.

Nicotinic acid protected germinal vesicle oocyte meiosis against toxicity of benzo(a)pyrene during maturation

Junjiu Huang (hjunjiu@mail.sysu.edu.cn)
School of Life Sciences, Sun Yat-sen University https://orcid.org/0000-0002-3417-1196
Min Gao
School of Life Sciences, Sun Yat-sen University
Dungao Li
The Reproduction Medicine Center of Hui Zhou Municipal Central Hospital
Shaoquan Zhan
Third Affiliated Hospital of Guangzhou Medical University
Yanling Qiu
School of Life Sciences, Sun Yat-sen University
Bohong Chen
School of Life Sciences, Sun Yat-sen University
Tianqi Cao
School of Life Sciences, Sun Yat-sen University
Zhiyun Chen
The Reproduction Medicine Center of Hui Zhou Municipal Central Hospital

Article

Keywords: benzo(a)pyrene, germinal vesicle oocyte, nicotinic acid, oxidative stress, in vitro maturation

Posted Date: November 18th, 2022

DOI: https://doi.org/10.21203/rs.3.rs-2236225/v1

License: This work is licensed under a Creative Commons Attribution 4.0 International License.
Read Full License

Abstract

Accumulating evidence has demonstrated that high concentration of benzo(a)pyrene (BaP) causes oocyte and embryo developmental arrest or death resulting in early pregnancy loss. However, whether the physiological concentration of BaP exposure affects GV oocyte maturation in exposure population remains unclear. Here, we evaluate the effects of human ovarian follicular fluid concentrations of BaP on mouse and human germinal vesicle (GV) oocyte maturation. Moreover, we examined whether nicotinic acid (NA) reversed GV meiotic failure caused by BaP during *in vitro* maturation (IVM). We used human ovarian follicular fluid concentrations of 5 nM BaP and/or a relatively high concentration of 50 nM group to treat GV oocytes during IVM in mice and human. We found 5 nM/50 nM BaP exposure significantly reduced first polar body extrusion during mouse GV oocytes maturation. Sirt1 protein expression decreased after BaP treatment in mouse oocytes. Moreover, BaP exposure disorganized spindle and chromosome arrangement, disrupted cortical actin cap, impaired mitochondrial redistribution, and caused DNA damage in IVM metaphase II (MII) mouse oocytes. Importantly, NA supplementation (15μM) increased Sirt1 expression and significantly rescued most of the abnormal effects. We then explored the effect of 5 nM BaP on human GV oocytes, a concentration close to that in human ovarian follicular fluid, and found that BaP caused GV meiotic failure by increasing mitochondrial membrane potential and markedly elevating reactive oxygen species (ROS) levels. Finally, we showed that 15 μM NA supplementation partially rescued human GV oocytes from the toxicity of 5 nM BaP during IVM. Our study indicates that physiological concentrations of BaP could seriously disrupt GV oocyte IVM and cause meiotic defects leading to oocyte arrest in both mice and humans. NA partially protects GV oocyte meiosis against BaP toxicity during IVM.

Introduction

Smoking is a global concern. Approximately 177 million women worldwide are smokers (1). It has been estimated that approximately 20.7% of women smoke between 25 and 44 years of age in the United States (2). Cigarette smoke is a documented reproductive toxicant, whose adverse effects include, but are not limited to ovarian failure (3, 4) and infertility (5–7). It is also established that nonsmokers with excessive exposure to tobacco smoke may have reproductive consequences as great as those observed in smokers (2). More than 4000 chemicals are present in cigarette smoke, and several of them exhibit toxic mutagenic and carcinogenic properties. Benzo(a)pyrene (BaP) is a representative pollutant and carcinogen (8). The main routes of BaP entry into the human body are tobacco smoke, coal tar, or grilled food.

Recently, the substantial toxicity of BaP to the female reproductive system has attracted increasing attention (9–11). BaP and its metabolites have been detected in the placenta, serum, and breast milk of pregnant women (12, 13). When pregnant women were exposed to BaP (2.27 mg / m3) in the air, DNA adducts increased in neonatal blood. These DNA adducts were formed by epoxide metabolites (BPDE) of BaP that were bound covalently to DNA and increased cell carcinogenic, teratogenic, mutagenic potential or death (14, 15). In addition, excessive levels of reactive oxygen species (ROS) cause redox imbalance

and mitochondrial dysfunction, ultimately leading to DNA damage, apoptosis, or aging (16–18). Women exposed to mainstream smoke had significantly higher levels of BaP (1.32 ± 0.68ng/ml, about 5nM) in follicular fluid compared to non-smoking (0.03 ± 0.01ng/ml) ones (19). Our previous study showed that this physiological concentration (5nM) of BaP can seriously disrupt mouse preimplantation embryo development by inducing DNA damage and cell death (20). Immature oocytes were present in follicular fluid before ovulation. It is important to study how BaP in follicular fluid affects germinal vesicle (GV) oocyte maturation in exposed populations. However, published research has used extremely high concentrations of BaP (50–250μM), which led to meiotic arrest of mouse or porcine oocytes (10, 21). Thus, the effect of the physiological concentration of BaP on GV oocyte maturation remains unclear. Furthermore, whether we can find small molecules to rescue its toxicity is important for the development of associated reproductive techniques.

BaP exposure leads to excessive levels of ROS, resulting in redox imbalance, mitochondrial dysfunction, and DNA damage, ultimately leading to reproductive problems (16–18). Antioxidant measures comprise the main approach used to address ovum hypoevolution caused by environmental pollutants. For example, N-acetyl-L-cysteine (NAC) reduced ROS generated during *in vitro* maturation (IVM), and this effect was compromised when SIRT1 was inhibited, indicating that silencing information regulator 2 related enzyme 1 (SIRT1) plays a key role against variations in redox states during IVM (22). In fact, the majority of the antioxidants used during IVM (such as melatonin, resveratrol) focused on detecting the protein levels of the NAD^+-dependent deacetylase SIRT1(23–25). NAD^+ not only accelerates the consumption of free radicals but also inhibits their production, which in turn maintains cellular free radical homeostasis. Loss of NAD^+ alters the NAD^+ /SIRT1 axis and disrupts mitochondrial homeostasis (26). Thus, NAD^+ supplementation has been adopted for improving oocyte quality by reducing oxidative stress damage. NAD^+ is synthesized through three pathways: the de novo pathway, Preiss-Handler pathway, or NAD^+ salvage pathway (27, 28). Of these, nicotinic acid (NA) is involved in NAD^+ synthesis in the Preiss-Handler pathway (27, 28). In this study, we explored whether NA administration could alleviate oxidative stress and protect against meiotic defects induced by BaP during IVM of GV oocytes.

Herein, we focused on the effects of 5 or 50 nM BaP on GV oocyte maturation in humans and mice (29). Our data demonstrate that BaP exposure disrupts redox homeostasis, which adversely affects maturation and quality in both mouse and human GV-MII development. NA supplementation significantly improved the quality of GV oocytes during IVM.

Results

BaP disrupted mouse GV oocyte meiosis and reduced Sirt1 protein levels during IVM

To investigate the toxic effects of BaP exposure on mouse oocyte maturation, we used 5 nM BaP and a relatively high concentration of 50 nM group to treat GV oocytes during IVM. As shown in Fig. 1, exposure

to 5 or 50 nM BaP prominently reduced the maturation rate (63.7% or 51.7%, respectively) compared with the control group (87%, Fig. 1A-C). Previous studies have found that 50 μM BaP disrupted mitochondrial distribution and function during porcine oocyte maturation (21). Mitochondrial dysfunction inevitably induces oxidative stress (30). Therefore, we evaluated whether oxidative stress increased in BaP-exposed oocytes. Living oocytes were stained with CM-H_2DCFDA to determine ROS levels. Relative quantification analysis of intensity of ROS fluorescence signals showed that they were markedly elevated in oocytes exposed to 5 nM (fluorescence intensity:29.21 ± 1.17) and 50 nM BaP (fluorescence intensity:36.53 ± 1.65) compared to control oocytes (fluorescence intensity:6.39 ± 0.52) (Fig. 1D, E).

SIRT1 is involved in regulating ROS homeostasis, stimulating antioxidant expression, repairing cell damage, and preventing cell dysfunction (22, 31). Di Emidio et al. reported that Sirt1 is downregulated under H_2O_2 stress in aged mouse oocytes (22). We found that BaP exposure significantly reduced Sirt1 protein levels in GV mouse oocytes (Fig. 1F). In support, it has been shown that the expression of SIRT1 is reduced, leading to spindle defects and chromosome misalignment, and disturbed redistribution of cortical granules and mitochondria in vitro-aged porcine oocytes (32). We investigated whether BaP exposure disrupted spindle organization and chromosome alignment during mouse oocyte maturation. To address this issue, spindle morphology and chromosome alignment of BaP-exposed oocytes were examined. Nearly 90% of MII oocytes in the control group had typical barrel-shaped spindles and an accurate alignment of chromosomes (Fig. 1G). In contrast, exposure to 5 nM BaP or 50 nM BaP significantly disrupted spindle formation (22.7% or 31.5%) compared with the control (Fig. 1H) and increase chromosome misaligned (26.4% or 34.8%) (Fig. 1I). Taken together, our data indicate that BaP exposure at physiological concentrations disrupted GV oocyte maturation in mice.

Nicotinic Acid Protected Mouse Gv Oocyte Ivm Against Bap Exposure

NA administration can elevate NAD^+ and Sirt1 levels in aged oocytes in vitro (33–35). Therefore, we explored whether NA could alleviate meiotic arrest induced by BaP exposure. As shown in Fig. 2A and Supplementary Fig. 1, NA was diluted to a series of concentrations (7.5, 15, 60μM) in culture medium containing 5 or 50 nM BaP. Our data showed that the maturation rate of oocytes exposed to BaP increased with NA supplementation. As shown in Fig. 2B and 2C, 15 μM NA significantly increased the first polar body extrusion in the 5 nM BaP (84.3%) and 50 nM BaP exposure groups (83.3%) compared to the other concentrations. Moreover, 60 μM NA did not obviously increase the oocyte maturation ratio in the 5 nM (81.3%) and 50 nM BaP exposure groups (78.7%) compared to 15μM NA. 15 μM and 60 μM NA treatment could yield similar results in the 5 nM and 50 nM BaP exposure groups. Therefore, 15μM NA treatment was used and called NA in further experiments. We found 15μM NA administration increased the expression level of Sirt1, which was similar to the control (Fig. 2D). In addition, lower ROS levels were observed in the 5nM BaP + NA group (7.31 ± 0.34) or 50nM BaP + NA group (7.179 ± 0.3481), as detected by fluorescence intensity quantification (Supplementary Fig. 2). Taken together, our data indicate that NA could, at least partially, rescue maturation of mouse GV oocytes treated with BaP.

Nicotinic Acid Rescued Mitochondrial Dysfunction And Dna Damage In Bap-treated Mice During Gv Oocyte Maturation

NA effectively reverted BaP-induced oxidative stress and reduced SIRT1 levels in mouse oocytes. Next, we examined whether NA could improve the subcellular structure abnormalities and DNA damage. Mitochondria are the most important subcellular structures in the oocyte cytoplasm that provide energy for oocyte maturation (36). MII oocytes were labeled with Mito Tracker to assess mitochondrial dynamics (Fig. 3A). Almost 80% of the MII oocytes in the control group showed typical accumulation of mitochondria at the spindle periphery. In contrast, we observed approximately 58.5% or 62.9% abnormal mitochondrial distribution in oocytes exposed to 5 nM or 50 nM BaP respectively (Fig. 3B). However, we found that ~ 22% of the abnormal distribution pattern was markedly decreased in the 5nM BaP + NA or 50nM BaP + NA groups compared with the BaP exposure. These results suggest that IVM supplemented with NA improves mitochondrial distribution and function. Next, we explored whether NA supplementation could improve subcellular structure abnormalities. Mitochondria provide energy for oocyte cytoskeletal organization. The markedly decreased abnormalities in spindle assembly and chromosome defects caused by 5 nM or 50 nM BaP are shown in Supplementary Fig. 3A. In particular, only 7.7% or 9.2% of abnormal spindles were detected in the 5 nM BaP + NA or 50 nM BaP + NA groups, respectively (Supplementary Fig. 3B). Similarly, a significant decrease in chromosome misalignment was found in both groups treated with NA (13.7% or 13.2%) (Supplementary Fig. 3C).

Actin filaments are essential for first polar body (Pb1) extrusion during oocyte meiosis (37). Next, we investigated whether BaP exposure caused changes in actin dynamics. F-actin was labeled with phalloidin (Fig. 3C). We found that there were strong signals of actin filaments on the membrane in the 5 nM BaP-treated oocytes (47.7%) and in the 50 nM BaP treatment (36%) groups compared to the control group (81.7%) (Fig. 3D). Notably, NA supplementation remarkably increased the intensity of signals of actin filaments in the 5 nM (78.5%) and 50 nM BaP treatment groups (74.8%) compared with the control group. These data suggest that NA restored spindle assembly and chromosome alignment and reversed actin filament defects induced by BaP exposure during mouse oocyte maturation.

High levels of oxidative stress can induce DNA damage. Thus, we examined whether exposure to 5 nM or 50 nM BaP induced DNA damage in MII oocytes (Fig. 3E). Our data demonstrated that γ-H2A.X signals were significantly increased following treatment of oocytes with 5 nM (fluorescence intensity:31.36 ± 2.34) and 50 nM (fluorescence intensity:35.72 ± 1.81) BaP relative to the control (fluorescence intensity:4.65 ± 0.66) (Fig. 3F). However, NA protected GV oocytes against DNA damage induced following exposure to 5 nM BaP (fluorescence intensity:6.57 ± 0.71) and 50 nM BaP (fluorescence intensity:6.34 ± 0.62), showing significantly decreased γ-H2A.X signals. Our results indicate that NA partly alleviated subcellular structure abnormalities and DNA damage in BaP-exposed mouse oocytes.

Nicotinic Acid Protected Human Gv Vesicle Oocyte Meiosis Against Toxicity Of Bap During Maturation

Women exposed to mainstream smoke have approximately 5 nM BaP in their follicular fluid (19). Thus, we explored the toxic effects of 5 nM BaP exposure on human GV oocyte maturation (Fig. 4A). Clinically discarded GV oocytes from intracytoplasmic sperm injection (ICSI) / in vitro fertilization (IVF) patients were used. Approximately 75% of GV oocytes extruded Pb1 in the control group, however, 5 nM BaP exposure significantly decreased the maturation rate of human GV oocytes (31.7%) (Fig. 4B, C). After 24–30 h of IVM, GV oocytes were stained with the fluorescent dye CM-H_2DCFDA to determine ROS levels. Consistent with the phenotype of mouse oocytes, treatment of human GV oocytes with 5 nM BaP (fluorescence intensity:26.43 ± 3.36) induced a significant increase in ROS levels compared to the control (fluorescence intensity:4.83 ± 1.18) (Fig. 4D, E). Because 15 μM NA could alleviate the impaired mouse oocyte quality caused by 5 nM or 50 nM BaP, we treated human GV oocytes exposed to 5nM BaP during IVM with 15μM NA (Fig. 4F). NA increased Pb1 extrusion in BaP-exposed oocytes (56.7%) compared with that in the control (71.3%) (Fig. 4G). Overall, these results suggest that BaP exposure inhibits human GV oocyte maturation, and 15 μM NA administration could rescue it. As expected, NA supplementation (fluorescence intensity:7.04 ± 0.30) significantly decreased ROS levels (Supplementary Fig. 4). Mitochondrial membrane potential is an important marker of mitochondrial function. To determine mitochondrial membrane potential, the oocytes were labeled with the fluorescent dye JC-1 (Fig. 4H). JC-1 monomers show more green fluorescence signals, whereas JC-1 aggregates gathered in the matrix of mitochondria show red fluorescence signals. The JC-1 red/green fluorescence ratio represents the membrane potential state. Human oocytes exposed to 5 nM BaP showed lower mitochondrial membrane potential, as indicated by the green fluorescence (JC-1 red/green fluorescent ratio 0.63), while the control group showed red fluorescence (JC-1 red/green fluorescent ratio 1.51). Importantly, NA supplementation significantly increased mitochondrial membrane potential (JC-1 red/green fluorescent ratio 1.04) (Fig. 4I). Taken together, these data indicate that NA improved the quality of BaP-exposed human GV oocytes in IVM.

Discussion

Our results demonstrated that exposure to the physiological concentration of BaP decreased mouse and human GV oocyte maturation, which was associated with increased ROS levels, and disruption of mitochondrial functions, spindle assembly, and chromosome arrangement. Importantly, we found that NA supplementation increased Sirt1 expression levels and reduced BaP toxicity during IVM.

Smoke produced by tobacco can be divided into mainstream smoke and side stream smoke. Active smokers inhale from the filter tip of the cigarette is called the mainstream smoke, smokers exhale mainstream smoke, side stream smoke, and the surrounding air mixed to form secondhand smoke. Gas chromatography-mass spectrometry was used to quantify BaP levels in the follicular fluid of women undergoing in vitro fertilization and exposed to mainstream smoke (n = 19) and non-smokers (n = 10). The concentration of BaP in the follicular fluid in women who smoke were approximately 5nM (38). Previous reports used pig or mouse models to determine the adverse impacts of BaP exposure during oocyte meiosis, and the concentrations used were much higher than the physiologic concentrations of

the exposed populations (approximately 50, 100 or 250μM) (10, 21). Considering the known reproductive toxicity of BaP, we used BaP concentrations present in the follicular fluid of smoking women, and a relatively high concentration of 50 nM group in mouse GV oocytes. The follicular fluid concentration of BaP could better simulate the physiological environment of human GV oocyte exposure. Therefore, only the effect of 5 nM BaP was on human GV oocyte maturation was examined. We obtained similar results between 5 nM and 50 nM BaP-exposed mouse oocytes and 5nM BaP-exposed human oocytes, including a decreased maturation rate and increased oxidative stress. Therefore, mouse GV oocytes could be a good study model for toxicity studies.

NAD^+ is one of the key molecules that controls mitochondrial oxidative metabolism during oocyte development (39). When released into the extracellular environment, it is also a substrate for a variety of signaling enzymes and regulates various cellular signaling pathways, including deacetylases (sirtuins), ADP ribosyl transferases, and circulating ADP ribose synthetases (40–42). Of these, Sirt1 is the NAD^+-dependent deacetylase, which is responsible for alleviating oxidative stress in ovarian cells through deacetylation of members of the fork head box transcription factor (FOXO) family (25, 43, 44). Sirt1 represents a front-line defense mechanism against ROS through the FoxO3a-MnSod axis in mouse GV oocyte maturation (45). Moreover, decreased Sirt1 levels lead to mitochondrial dysfunction by increasing ROS, lipid peroxidation, and DNA damage in oocytes, and thereby resulting in infertility (46). Several antioxidant supplements that improve mitochondrial function in vitro have been shown to increasing the developmental competence of oocytes or embryos (47). Consistent with this notion, we found that Sirt1 expression decreased following treatment of mouse oocytes with physiological concentrations of BaP. We also used Sirt1 protein expression levels to evaluate oocyte quality.

Sirt1 serves as a universal mediator that exerts metabolic effects in a tissue-dependent manner in response to changes in the systemic levels of NAD^+ (48). Therefore, NAD^+ supplementation can be used to decrease oocyte ROS levels (33–35). Nicotinic acid administration during in vitro culture improves oocyte quality by elevating NAD^+ and Sirt1 levels in aged oocytes (27). Collins et al. reported that NA is a more favorable precursor than nicotinamide (NAM) in the liver, intestine, and kidneys (49). In addition, NA treatment had a more favorable action in correcting meiosis in high-fat diet (HFD) mouse oocytes compared to nicotinamide mononucleotide (NMN) (50). Since NA is more effective when supplemented in vitro, we selected NA to supplement NAD^+ and evaluated the effect of NA by detecting Sirt1 protein levels. Our data also showed that NA supplementation restored Sirt1 levels, lowered ROS production, and ameliorated meiotic defects in BaP-exposed mouse oocytes. Importantly, NA not only improved human oocyte maturation but also protected against mitochondrial dysfunction and oxidative stress in BaP-treated GV oocytes.

In a follow-up study, we aim to evaluate the effect of BaP exposure on the developmental potential of the embryo and after the effects of NA treatment. This study provides a new approach for improving human GV oocyte IVM clinical outcomes in assisted reproduction. In addition, it suggests NA supplementation to

improve oocyte quality during assisted reproduction in patients who are active or passive smokers, thus, improve reproductive outcomes in these populations.

Materials And Methods

All chemicals and culture media were purchased from Sigma (St. Louis, MO, USA) unless stated otherwise.

Animal Care And Ethics Statement

In mouse part, CD1 mice were used in this study. Protocols were approved by the Animal Care and Use Committee of Sun-Yat-Sen University, and performed according to the institutional Animal Care and Use Committee of Sun Yat-Sen University, People's Republic of China. CD1 mice were used 6-8week-old female mice in this study.

In human part, the study was approved by the Committee of Medical Ethics. All patients in this study had written their informed consent. Germinal vesicle (GV) oocytes collection was conducted at the Hospital of Huizhou Reproductive Medicine Center.

Gv Oocytes Collection And Culture

In mouse part, CD1 mice were used for oocyte collection in this study. To collect fully grown germinal vesicle (GV) oocytes, mice were super ovulated with 5 IU Pregnant Mares Serum Gonadotropin (PMSG) by intraperitoneal injection. For in vitro maturation, oocytes were cultured in M2 medium about 14 hours under liquid paraffin oil at 37°C in a 5% CO_2 atmosphere.

In human part, GV oocytes were clinically useless, these are typically discarded according to the policy of IVF program. The discarded immature oocytes were only released for this research if patients had signed an informed consent for use of their discarded materials. The study used immature oocytes that had been aspirated during oocyte retrieval from patients undergoing IVF/ICSI patients between May 2019 and May 2022 in our IVF program. 78 human oocytes were collected over 2 years (35 years). The human GV oocytes were frozen (VT101) and unfrozen (VT102) according to the instructions of the reagents. The freezing process was carried out by doctors in the Reproduction Medicine Center of Hui Zhou Municipal Central Hospital, then stored in a liquid nitrogen tank, and transported to the laboratory of the School of Life Sciences, Sun Yat-sen University. Before the experiment, the unfrozen operation was performed. Then, the immature oocytes were cultured in vitro in G-IVF PLUS medium about 24–30 hours under liquid paraffin oil at 37°C in a 5% CO_2 atmosphere.

Bap And Na Treatment

In mouse part, BaP dissolved in DMSO was diluted in M2 medium to produce a final concentration of 5nM and 50nM respectively. The negative control group added the same amount of DMSO, called CTRL group. NA was dissolved in 5nM or 50nM BaP contaminated culture medium to yield a final concentration of 7.5μM,15μM,60μM.

In human immature part, BaP dissolved in DMSO was diluted in G-IVF PLUS medium to produce a final concentration of 5nM. The control group added the same amount of DMSO. NA was dissolved in 5nM BaP contaminated culture medium to yield a final concentration of 15μM.

Antibodies

Rabbit polyclonal anti-Sirt1 antibody was purchased from Abcam (Cat#: ab32441); Rabbit polyclonal anti-gamma H2A.X (phosphor-S139) antibody was purchased from Abcam (Cat#: ab2893).

Western Blotting

100 mouse oocytes were lysed in laemmli sample buffer with protease inhibitor and boiled for 5 minutes. The specific experimental operations were based on our pre-published protocol (51, 52).

Immunofluorescence

The specific operations were based on our pre-published protocol (51, 52). Samples were mounted on anti-fade medium and examined under a Laser Scanning Confocal Microscope.

Mitochondria Distribution Measurement

Mito Tracker was labeled the mitochondria. Living oocytes were cultured in M2 medium containing 200 nM Mito Tracker Red (Molecular Probes, Eugene, OR) for 30 min at 37°C.

Mitochondrial Membrane Potential Measurement

Oocytes were cultured in M2 medium containing 2μM JC-1 (Thermo Fisher Scientific, Cat#: T3168) for 30 min at 37°C. The chromosomes were counterstained with propidium iodide (PI) or Hoechst33342 for 10 minutes. Oocytes were transferred to a live cell-imaging dish after 3 washes. Fluorescence was detected by a Leica inverted microscope.

Ros Measurement

Living oocytes were incubated in M2 medium with 5μM CM-H2DCFDA (Life Technologies, Invitrogen TM, Cat#:C6827) for 30 min at 37°C in 5% CO_2 atmosphere. Oocytes were transferred to a live cell-imaging dish after 3 washes, and observed using a Confocal Microscope.

Statistical analysis

Data were showed as mean ± SEM. Statistical comparisons were used Student's t test and analyzed were performed using GraphPad Prism software.

Declarations

Funding Statement: This study was funded by the National Natural Science Foundation of China (82271688 and 31971365) and the Hui Zhou Municipal Central Hospital Deng feng Project of Guangdong (2019–2022).

Disclosure Statement: The authors declare that they have no conflict of interest.

Attestation Statement:

• Data regarding any of the subjects in the study has not been previously published.

• Data will be made available to the editors of the journal for review or query upon request.

Data Sharing Statement: All data generated or analyzed during this study are available from the corresponding author on reasonable request.

Ethics declarations

Conflict of interest

The authors declare that they have no conflict of interest.

Author's contributions

JH and ZC conceived and designed the project. MG, DL SZ YQ BC and TC performed the experiments. MG, DL SZ YQ BC, TC, ZC and JH analyzed the data. JH and MG wrote the manuscript. JH and ZC contributed to the final approval of the manuscript. All authors read and approved the final manuscript.

Supplementary information is available at *Cell Death Discovery*'s website.

References

1. Jamal A, Agaku IT, O'Connor E, King BA, Kenemer JB, Neff L. Current cigarette smoking among adults–United States, 2005-2013. MMWR Morb Mortal Wkly Rep. 2014;63(47):1108-12.

2. Practice Committee of the American Society for Reproductive Medicine. Electronic address aao, Practice Committee of the American Society for Reproductive M. Smoking and infertility: a committee opinion. Fertil Steril. 2018;110(4):611-8.
3. Lim J, Lawson GW, Nakamura BN, Ortiz L, Hur JA, Kavanagh TJ, et al. Glutathione-deficient mice have increased sensitivity to transplacental benzo[a]pyrene-induced premature ovarian failure and ovarian tumorigenesis. Cancer Res. 2013;73(2):908-17.
4. Gannon AM, Stampfli MR, Foster WG. Cigarette smoke exposure leads to follicle loss via an alternative ovarian cell death pathway in a mouse model. Toxicol Sci. 2012;125(1):274-84.
5. Radin RG, Hatch EE, Rothman KJ, Mikkelsen EM, Sorensen HT, Riis AH, et al. Active and passive smoking and fecundability in Danish pregnancy planners. Fertil Steril. 2014;102(1):183-91 e2.
6. Waylen AL, Metwally M, Jones GL, Wilkinson AJ, Ledger WL. Effects of cigarette smoking upon clinical outcomes of assisted reproduction: a meta-analysis. Human reproduction update. 2009;15(1):31-44.
7. Neal MS, Hughes EG, Holloway AC, Foster WG. Sidestream smoking is equally as damaging as mainstream smoking on IVF outcomes. Hum Reprod. 2005;20(9):2531-5.
8. Budani MC, Tiboni GM. Ovotoxicity of cigarette smoke: A systematic review of the literature. Reprod Toxicol. 2017;72:164-81.
9. Ye X, Pan W, Li C, Ma X, Yin S, Zhou J, et al. Exposure to polycyclic aromatic hydrocarbons and risk for premature ovarian failure and reproductive hormones imbalance. J Environ Sci (China). 2020;91:1-9.
10. Zhang M, Miao Y, Chen Q, Cai M, Dong W, Dai X, et al. BaP exposure causes oocyte meiotic arrest and fertilization failure to weaken female fertility. FASEB J. 2018;32(1):342-52.
11. Einaudi L, Courbiere B, Tassistro V, Prevot C, Sari-Minodier I, Orsiere T, et al. In vivo exposure to benzo(a)pyrene induces significant DNA damage in mouse oocytes and cumulus cells. Hum Reprod. 2014;29(3):548-54.
12. Al-Saleh I, Alsabbahen A, Shinwari N, Billedo G, Mashhour A, Al-Sarraj Y, et al. Polycyclic aromatic hydrocarbons (PAHs) as determinants of various anthropometric measures of birth outcome. Sci Total Environ. 2013;444:565-78.
13. Madhavan ND, Naidu KA. Polycyclic aromatic hydrocarbons in placenta, maternal blood, umbilical cord blood and milk of Indian women. Hum Exp Toxicol. 1995;14(6):503-6.
14. Borman SM, Christian PJ, Sipes IG, Hoyer PB. Ovotoxicity in female Fischer rats and B6 mice induced by low-dose exposure to three polycyclic aromatic hydrocarbons: comparison through calculation of an ovotoxic index. Toxicol Appl Pharmacol. 2000;167(3):191-8.
15. Sadeu JC, Foster WG. Cigarette smoke condensate exposure delays follicular development and function in a stage-dependent manner. Fertil Steril. 2011;95(7):2410-7.
16. Sobinoff AP, Pye V, Nixon B, Roman SD, McLaughlin EA. Jumping the gun: smoking constituent BaP causes premature primordial follicle activation and impairs oocyte fusibility through oxidative stress. Toxicol Appl Pharmacol. 2012;260(1):70-80.

17. Keating AF, Fernandez SM, Mark-Kappeler CJ, Sen N, Sipes IG, Hoyer PB. Inhibition of PIK3 signaling pathway members by the ovotoxicant 4-vinylcyclohexene diepoxide in rats. Biol Reprod. 2011;84(4):743-51.
18. Dumollard R, Carroll J, Duchen MR, Campbell K, Swann K. Mitochondrial function and redox state in mammalian embryos. Semin Cell Dev Biol. 2009;20(3):346-53.
19. Neal MS, Zhu J, Foster WG. Quantification of benzo[a]pyrene and other PAHs in the serum and follicular fluid of smokers versus non-smokers. Reprod Toxicol. 2008;25(1):100-6.
20. Zhan S, Zhang X, Cao S, Huang J. Benzo(a)pyrene disrupts mouse preimplantation embryo development. Fertil Steril. 2015;103(3):815-25.
21. Miao Y, Zhou C, Bai Q, Cui Z, ShiYang X, Lu Y, et al. The protective role of melatonin in porcine oocyte meiotic failure caused by the exposure to benzo(a)pyrene. Hum Reprod. 2018;33(1):116-27.
22. Di Emidio G, Falone S, Vitti M, D'Alessandro AM, Vento M, Di Pietro C, et al. SIRT1 signalling protects mouse oocytes against oxidative stress and is deregulated during aging. Hum Reprod. 2014;29(9):2006-17.
23. Tamura H, Nakamura Y, Takiguchi S, Kashida S, Yamagata Y, Sugino N, et al. Melatonin directly suppresses steroid production by preovulatory follicles in the cyclic hamster. J Pineal Res. 1998;25(3):135-41.
24. Lan M, Han J, Pan MH, Wan X, Pan ZN, Sun SC. Melatonin protects against defects induced by deoxynivalenol during mouse oocyte maturation. J Pineal Res. 2018;65(1):e12477.
25. Nishigaki A, Tsubokura H, Tsuzuki-Nakao T, Okada H. Hypoxia: Role of SIRT1 and the protective effect of resveratrol in ovarian function. Reprod Med Biol. 2022;21(1):e12428.
26. Croteau DL, Fang EF, Nilsen H, Bohr VA. NAD(+) in DNA repair and mitochondrial maintenance. Cell Cycle. 2017;16(6):491-2.
27. Wu X, Hu F, Zeng J, Han L, Qiu D, Wang H, et al. NMNAT2-mediated NAD(+) generation is essential for quality control of aged oocytes. Aging Cell. 2019;18(3):e12955.
28. Lundt S, Ding S. NAD(+) Metabolism and Diseases with Motor Dysfunction. Genes (Basel). 2021;12(11).
29. Neal MS, Zhu J, Holloway AC, Foster WG. Follicle growth is inhibited by benzo-[a]-pyrene, at concentrations representative of human exposure, in an isolated rat follicle culture assay. Hum Reprod. 2007;22(4):961-7.
30. Adhikari D, Lee IW, Yuen WS, Carroll J. Oocyte mitochondria-key regulators of oocyte function and potential therapeutic targets for improving fertility. Biol Reprod. 2022;106(2):366-77.
31. Singh CK, Chhabra G, Ndiaye MA, Garcia-Peterson LM, Mack NJ, Ahmad N. The Role of Sirtuins in Antioxidant and Redox Signaling. Antioxid Redox Signal. 2018;28(8):643-61.
32. Ma R, Zhang Y, Zhang L, Han J, Rui R. Sirt1 protects pig oocyte against in vitro aging. Anim Sci J. 2015;86(9):826-32.

33. Nadeeshani H, Li J, Ying T, Zhang B, Lu J. Nicotinamide mononucleotide (NMN) as an anti-aging health product - Promises and safety concerns. Journal of advanced research. 2022;37:267-78.
34. Miao Y, Cui Z, Gao Q, Rui R, Xiong B. Nicotinamide Mononucleotide Supplementation Reverses the Declining Quality of Maternally Aged Oocytes. Cell reports. 2020;32(5):107987.
35. Bertoldo MJ, Listijono DR, Ho WJ, Riepsamen AH, Goss DM, Richani D, et al. NAD(+) Repletion Rescues Female Fertility during Reproductive Aging. Cell reports. 2020;30(6):1670-81.e7.
36. Scantland S, Tessaro I, Macabelli CH, Macaulay AD, Cagnone G, Fournier É, et al. The adenosine salvage pathway as an alternative to mitochondrial production of ATP in maturing mammalian oocytes. Biol Reprod. 2014;91(3):75.
37. Shan MM, Sun SC. The multiple roles of RAB GTPases in female and male meiosis. Human reproduction update. 2021;27(6):1013-29.
38. Tuttle AM, Stampfli M, Foster WG. Cigarette smoke causes follicle loss in mice ovaries at concentrations representative of human exposure. Hum Reprod. 2009;24(6):1452-9.
39. Miranda-Vizuete A, Damdimopoulos AE, Spyrou G. The mitochondrial thioredoxin system. Antioxid Redox Signal. 2000;2(4):801-10.
40. Yang Y, Sauve AA. NAD(+) metabolism: Bioenergetics, signaling and manipulation for therapy. Biochim Biophys Acta. 2016;1864(12):1787-800.
41. Johnson S, Imai SI. NAD (+) biosynthesis, aging, and disease. F1000Res. 2018;7:132.
42. Hamaidi I, Kim S. Sirtuins are crucial regulators of T cell metabolism and functions. Exp Mol Med. 2022;54(3):207-15.
43. Hori YS, Kuno A, Hosoda R, Horio Y. Regulation of FOXOs and p53 by SIRT1 modulators under oxidative stress. PLoS One. 2013;8(9):e73875.
44. Iyer S, Han L, Bartell SM, Kim HN, Gubrij I, de Cabo R, et al. Sirtuin1 (Sirt1) promotes cortical bone formation by preventing β-catenin sequestration by FoxO transcription factors in osteoblast progenitors. J Biol Chem. 2014;289(35):24069-78.
45. Lin CH, Lin CC, Ting WJ, Pai PY, Kuo CH, Ho TJ, et al. Resveratrol enhanced FOXO3 phosphorylation via synergetic activation of SIRT1 and PI3K/Akt signaling to improve the effects of exercise in elderly rat hearts. Age (Dordr). 2014;36(5):9705.
46. Alam F, Syed H, Amjad S, Baig M, Khan TA, Rehman R. Interplay between oxidative stress, SIRT1, reproductive and metabolic functions. Curr Res Physiol. 2021;4:119-24.
47. Xu W, Li L, Sun J, Zhu S, Yan Z, Gao L, et al. Putrescine delays postovulatory aging of mouse oocytes by upregulating PDK4 expression and improving mitochondrial activity. Aging (Albany NY). 2018;10(12):4093-106.
48. Imai S. The NAD World: a new systemic regulatory network for metabolism and aging–Sirt1, systemic NAD biosynthesis, and their importance. Cell Biochem Biophys. 2009;53(2):65-74.
49. Collins PB, Chaykin S. The management of nicotinamide and nicotinic acid in the mouse. J Biol Chem. 1972;247(3):778-83.

50. Wang H, Zhu S, Wu X, Liu Y, Ge J, Wang Q, et al. NAMPT reduction-induced NAD(+) insufficiency contributes to the compromised oocyte quality from obese mice. Aging Cell. 2021;20(11):e13496.
51. He Y, Li X, Gao M, Liu H, Gu L. Loss of HDAC3 contributes to meiotic defects in aged oocytes. Aging Cell. 2019;18(6):e13036.
52. Gao M, Li X, He Y, Han L, Qiu D, Ling L, et al. SIRT7 functions in redox homeostasis and cytoskeletal organization during oocyte maturation. FASEB J. 2018:fj201800078RR.

Figures

Figure 1

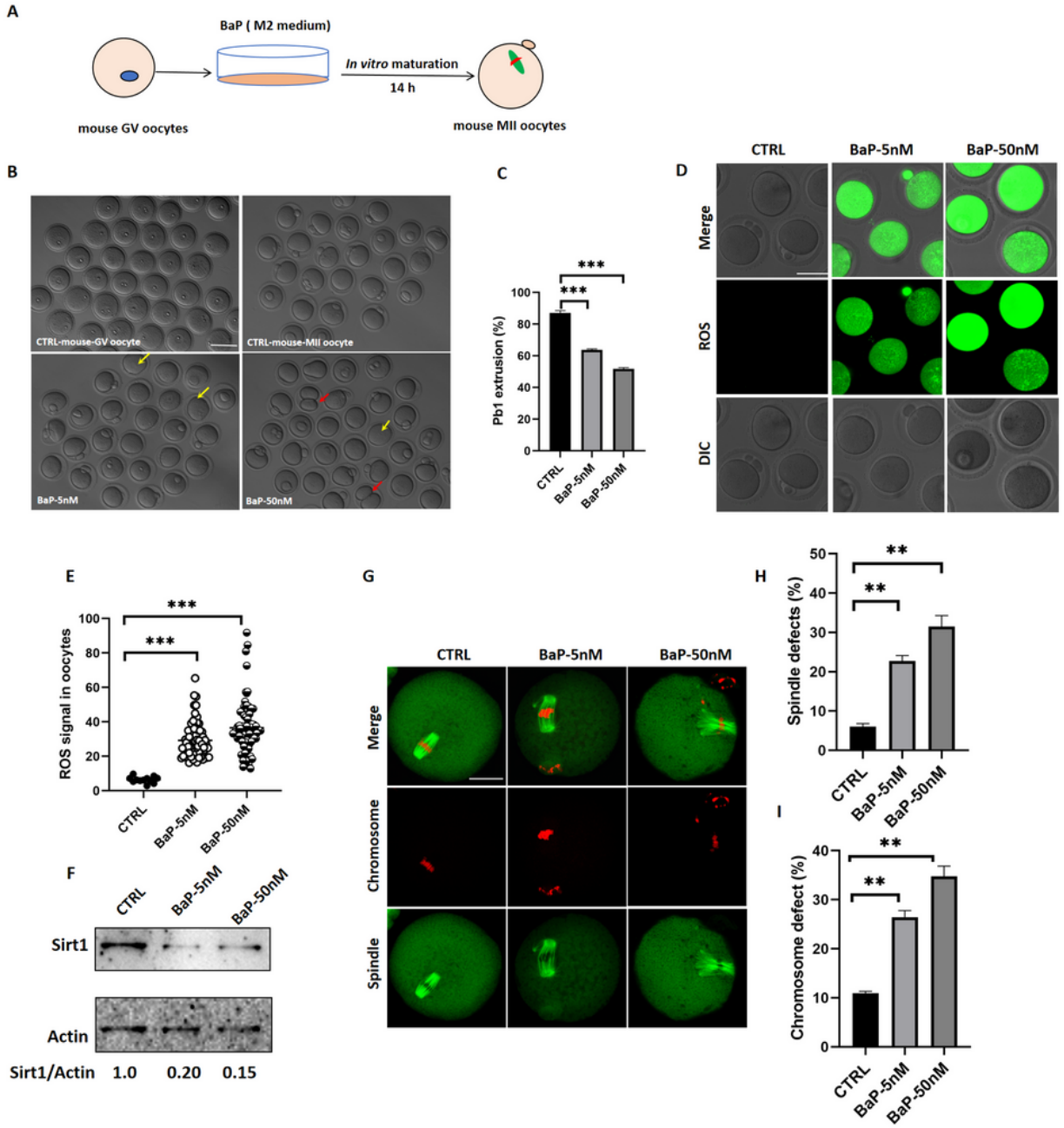

Figure 1

Effects of BaP exposure on the mouse oocyte maturation in vitro. (A) Schematic presentation of the experimental protocol in mouse oocytes. (B) Representative oocytes morphologies in different groups. Red arrowheads point to oocytes with symmetrical division or a large polar body. Yellow arrows point to oocytes with no polar body. Scale bar :80 μm. (C) The oocytes maturation rate in the control (n=199), BaP-5nM (n=176); BaP-50nM (n=196). BaP, Benzo(a)pyrene. (D) Representative images of CM-H_2DCFDA

fluorescence. Scale bar: 25 μm. (E) Quantification of the relative levels of ROS in control (n=12), BaP-5nM (n=73), BaP-50nM (n=81). Each data point represents an oocyte. (F) Sirt1 protein was verified by western blot analysis in different groups. The relative amount of Sirt1 was estimated based on the level of actin. (G) Oocytes were stained with α-tubulin antibody to visualize the spindle (green) and counterstained with Hoechst 33342 (red) for chromosomes. Representative images of spindle morphologies and chromosome alignment in the control, BaP-5nM, BaP-50nM treated oocytes. Scale bar: 25 μm. (H) Quantification of control (n=131), BaP-5nM (n=246), BaP-50nM (n=262) with spindle disorganization. (I) Quantification of control (n=137), BaP-5nM (n=192), BaP-50nM (n=180) with chromosome defects. Data were showed as mean percentage ± SEM of three independent experiments. *p < 0.05. **p < 0.01. ***p < 0.001.

Figure 2

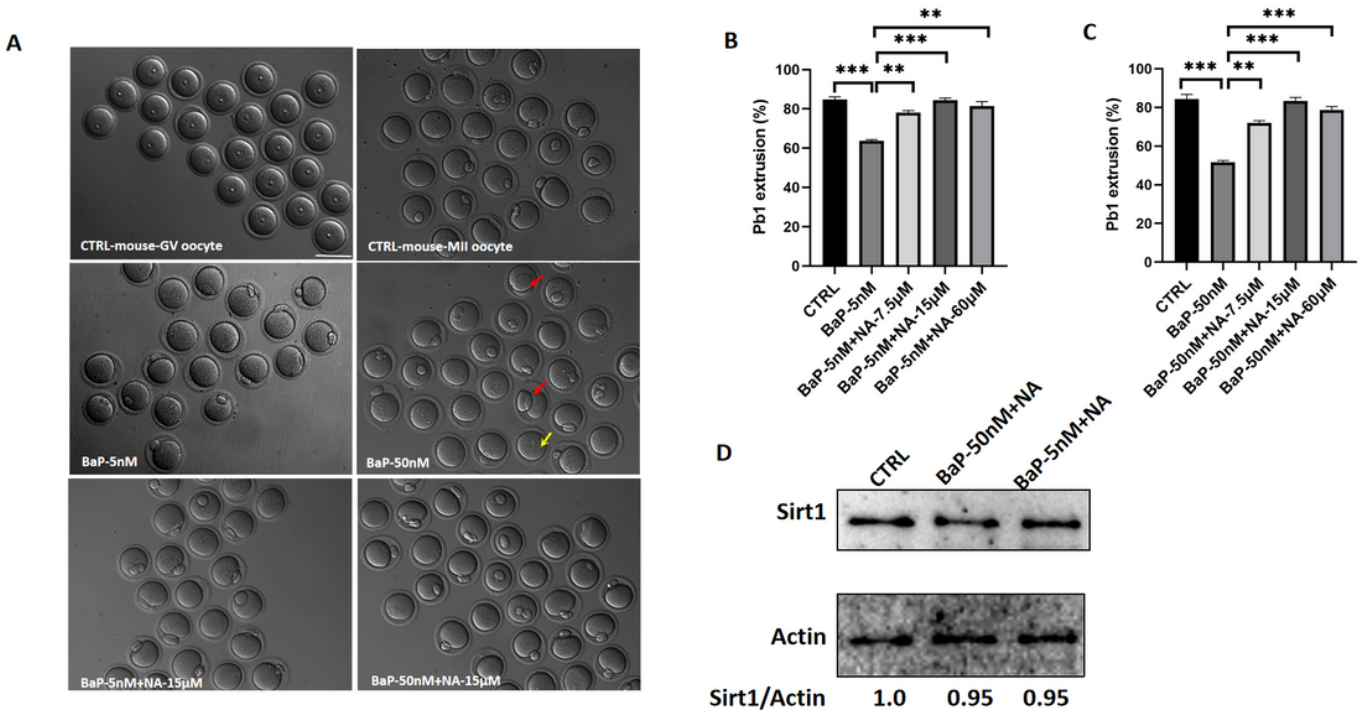

Figure 2

NA protected against meiotic maturation in BaP exposure mouse oocytes.

(A) Representative oocytes morphologies in different groups. Red arrowheads point to oocytes with symmetrical division or a large polar body. Yellow arrows point to oocytes with no polar body. Scale bar :80 μm. (B) NA protected against meiotic maturation in 5nM BaP exposure mouse oocytes. The oocytes maturation rate in control (n=112), BaP-5nM (n=120), BaP-5nM+NA-7.5μM (n=191), BaP-5nM+NA-15μM

(n=173), BaP-5nM+NA-60μM (n=154). (C) NA protected against meiotic maturation in 50nM BaP exposure mouse oocytes. The oocytes maturation rate in the control (n=89), BaP-50nM (n=162), BaP-50nM+NA-7.5μM (n=140), BaP-50nM+NA-15μM (n=175), BaP-50nM+NA-60μM (n=160). NA, nicotinic acid. (D) Sirt1 protein was verified by western blot analysis in different groups. The relative amount of Sirt1 was estimated based on the level of actin. Data were showed as mean percentage ± SEM of three independent experiments. *p < 0.05. **p < 0.01. ***p < 0.001.

Figure 3

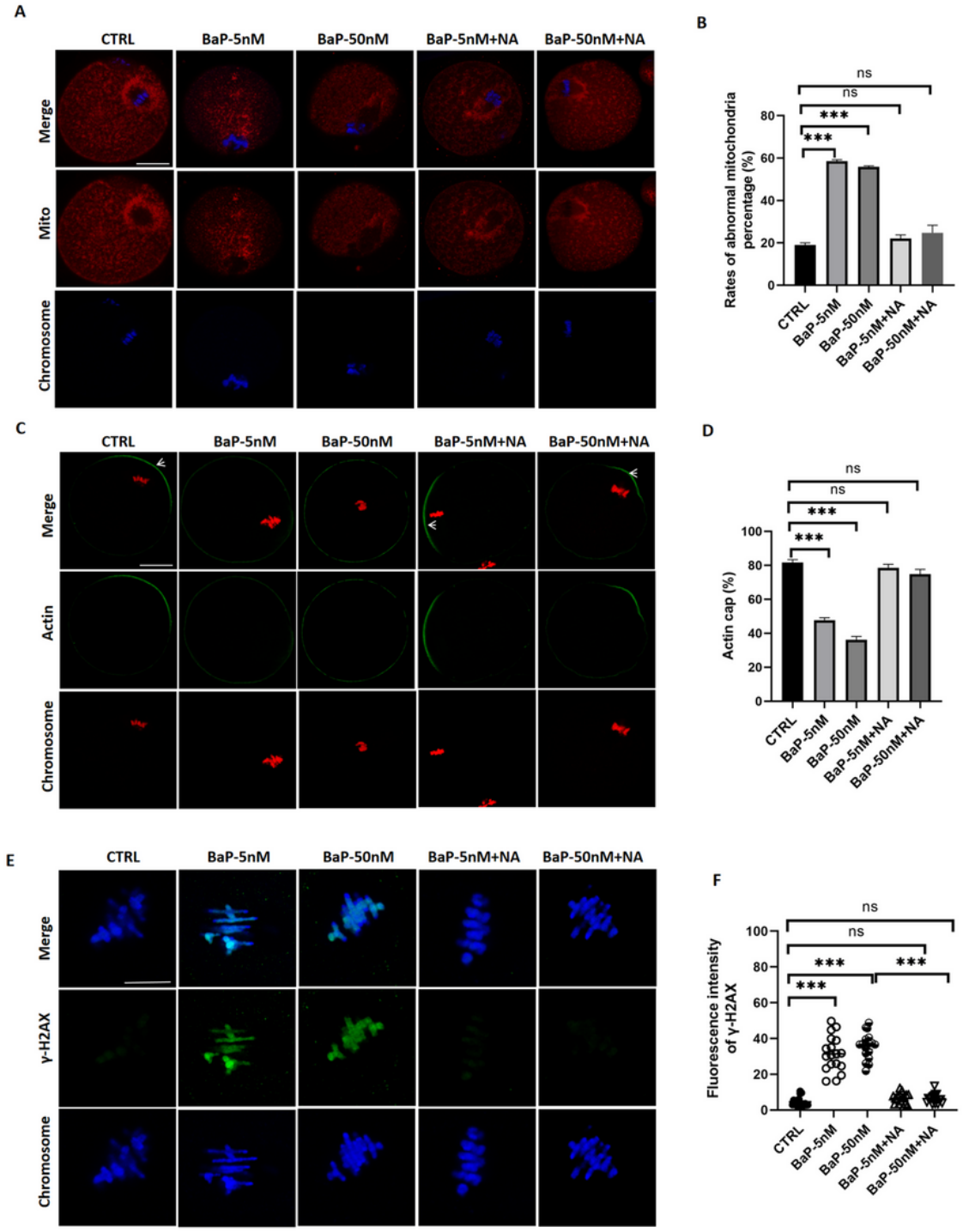

Figure 3

Effects of NA on the subcellular structure in BaP-exposed mouse oocytes. (A) Oocytes were labeled with Mito tracker Red to visualize mitochondrial distribution and counterstained with Hoechst 33342 (blue) for chromosomes. Representative images of mitochondrial distribution patterns in MII oocytes. Scale bar: 25μm. (B) Quantification of control (n=180), BaP-5nM (n=125), BaP-50nM (n=101), BaP-5nM+NA (n=81), BaP-50nM+NA (n=84) with each mitochondrial distribution pattern. (C) MII oocytes were labeled with phalloidin to visualize actin (green) and were counterstained with propidium iodide (PI) (red) for chromosomes. White arrowheads point to MII oocytes with actin filaments on the membrane. Scale bar: 25μm. (D) Quantitative analysis of control (n=115), BaP-5nM (n=120), BaP-50nM (n=126), BaP-5nM+NA (n=124), BaP-50nM+NA (n=141) with normal actin cap formation. (E) MII oocytes were stained with anti-γH2AX antibody to visualize DNA damage (green) and counterstained with Hoechst 33342 (blue) for chromosomes. Scale bar: 50 μm. (F) Quantitation of the fluorescence intensity of DNA damage number of DNA damage in control (n=17), BaP-5nM (n=18), BaP-50nM (n=17), BaP-5nM+NA (n=17), BaP-50nM+NA (n=17). Data were showed as mean percentage ± SEM of three independent experiments. *$p < 0.05$. **$p < 0.01$. ***$p < 0.001$.

Figure 4

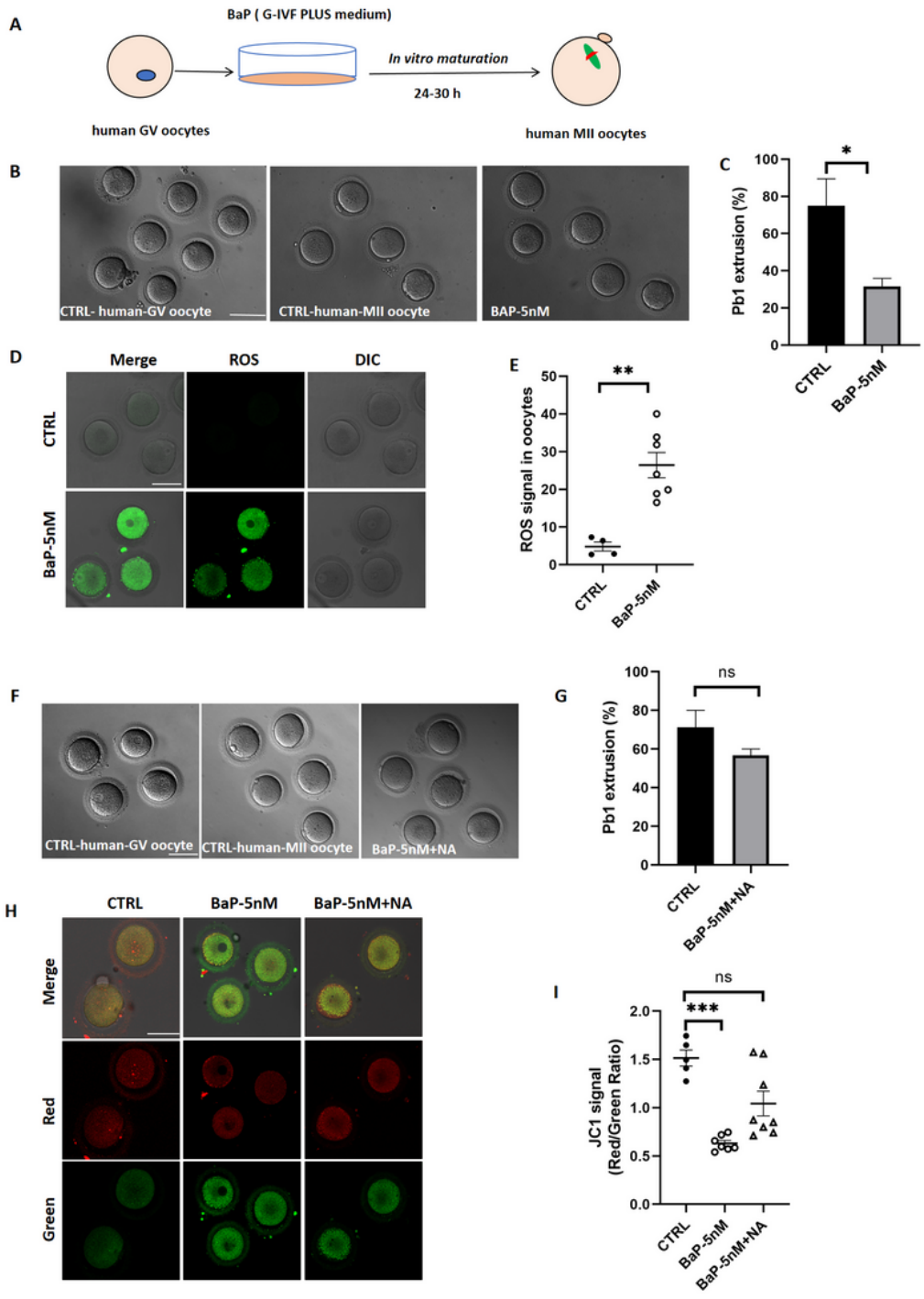

Figure 4

NA protected against meiotic maturation in BaP exposure human oocytes. (A) Schematic presentation of the experimental protocol in human oocytes. (B) Representative oocytes morphologies in different groups. Scale bar :100 μm. (C) The oocytes maturation rate in control (n=8), BaP-5nM (n=22). (D) Representative images of CM-H_2DCFDA fluorescence. Scale bar :30 μm (E) The fluorescence intensity of ROS in control (n=4), BaP-5nM (n=7). Each data point represents an oocyte. (F) Representative oocytes

morphologies in different groups. Scale bar :100 μm. (G) The oocytes maturation rate in control (n=13), BaP-5nM (n=16), BaP-5nM+NA (n=16). (H) Mitochondrial membrane potential measured by JC-1 fluorescence. The green fluorescence were inactive mitochondria and the red fluorescence were active mitochondria in oocytes. Scale bar :30 μm. (I) Histogram showing the JC-1 red/green fluorescence ratio control (n=5), BaP-5nM (n=7), BaP-5nM+NA (n=8). Each data point represents an oocyte. Data were showed as mean percentage ± SEM of three independent experiments. *p < 0.05. **p < 0.01. ***p < 0.001.

Supplementary Files

This is a list of supplementary files associated with this preprint. Click to download.

- SupplementaryFigure1.tif
- SupplementaryFigure2.tif
- SupplementaryFigure3.tif
- SupplementaryFigure4.tif
- SupplementaryMaterial.docx